Molecular Microbiology (2019) 111(5), 1317–1334

doi:10.1111/mmi.14223
First published online 26 March 2019

The master quorum-sensing regulators LuxR/HapR directly interact with the alpha subunit of RNA polymerase to drive transcription activation in *Vibrio harveyi* and *Vibrio cholerae*

Alyssa S. Ball and Julia C. van Kessel *
Department of Biology, Indiana University, Bloomington, IN 47405, USA.

Summary

In Vibrio species, quorum sensing controls gene expression for numerous group behaviors, including bioluminescence production, biofilm formation, virulence factor secretion systems, and competence. The LuxR/HapR master quorum-sensing regulators activate expression of hundreds of genes in response to changes in population densities. The mechanism of transcription activation by these TetR-type transcription factors is unknown, though LuxR DNA binding sites that lie in close proximity to the –35 region of the promoter are required for activation at some promoters. Here, we show that Vibrio harveyi LuxR directly interacts with RNA polymerase to activate transcription of the luxCDABE bioluminescence genes. LuxR interacts with RNA polymerase in vitro and in vivo and specifically interacts with both the N- and C-terminal domains of the RNA polymerase α-subunit. Amino acid substitutions in the RNAP interaction domain on LuxR decrease interactions between LuxR and the α-subunit and result in defects in transcription activation of quorum-sensing genes in vivo. The RNAP-LuxR interaction domain is conserved in Vibrio cholerae HapR and is required for activation of the HapR-regulated gene hapA. Our findings support a model in which LuxR/HapR bind proximally to RNA polymerase to drive transcription initiation at a subset of quorum-sensing genes in Vibrio species.

Accepted 6 February, 2019. *For correspondence. E-mail jcvk@indiana.edu; Tel. (+1)812-856-2235; Fax 812-856-5710.

Introduction

Bacterial communication is central to the regulation of various developmental processes, including biofilm formation, virulence factor secretion, competence and bioluminescence (Rutherford and Bassler, 2012). Intra- and interspecies communication, called quorum sensing, directs population-wide changes in gene expression through release and detection of signaling molecules called autoinducers. Autoinducers convey the number and type of cells within their vicinity; as the concentration of autoinducers changes, bacteria alter gene expression to coordinate behaviors.

In many Vibrio species, autoinducers are detected via membrane-bound histidine kinase receptors that initiate a phosphorylation cascade upon autoinducer binding (Ng and Bassler, 2009; Hawver et al., 2016). This signaling pathway culminates in expression of the master quorum-sensing regulator, which is called LuxR in Vibrio harveyi (Ball et al., 2017). LuxR homologs are highly conserved in Vibrios and all act as the master quorum-sensing regulators, including HapR in Vibrio cholerae, SmcR in Vibrio vulnificus, OpaR in Vibrio parahaemolyticus, VanT in Vibrio anguillarum and VtpR in Vibrio tubiashii. At low cell densities, autoinducer concentrations are low, resulting in low expression of the master quorum-sensing regulator, LuxR. At high cell densities, autoinducer concentrations are high, resulting in maximal expression of LuxR. LuxR expression increases 10-fold between low cell density and high cell density, producing a global change in the quorum-sensing gene network via activation and repression of downstream genes ranging 2- to 200-fold (Waters and Bassler, 2006; van Kessel et al., 2013b).

Although the V. harveyi master transcription regulator is named LuxR, it has a distinct structure and function compared to the LuxR proteins that bind autoinducers in typical LuxI/LuxR quorum-sensing systems of Gram-negative bacteria (e.g. the LuxR present in Vibrio fischeri) (Ball et al., 2017). The master quorum-sensing factor LuxR in V. harveyi, suffering from confusing nomenclature, is actually a member of the TetR family of transcription factors and is distinct from V. fischeri LuxR at the molecular,

genetic and biochemical levels (Pompeani et al., 2008; van Kessel et al., 2013b). V. fischeri, which encodes a canonical LuxI/LuxR system, also has a LuxR/HapR homolog called LitR that functions upstream of LuxR in its quorum-sensing system (Fidopiastis et al., 2002; Studer et al., 2008). V. harveyi LuxR-type proteins are structurally conserved among vibrios and share high amino acid identity with the master regulators in other species: 71% with HapR (V. cholerae), 96% with OpaR (V. parahaemolyticus), 93% with SmcR (V. vulnificus) and 60% with LitR (V. fischeri). LuxR proteins function as dimers and have a similar structure to TetR but are distinct from most other TetR proteins in their function (Ramos et al., 2005). LuxR family proteins can both activate and repress hundreds of quorum sensing-regulated genes, whereas TetR-type proteins typically act only as repressors and regulate 1 or 2 genes. In V. harveyi, the LuxR regulon is 625 genes, and LuxR binds to multiple binding sites within the promoter regions of genes it directly regulates (van Kessel et al., 2013a; 2013b), unlike many characterized TetR-type proteins that regulate their promoters by binding to a single binding site. For example, there are eight LuxR binding sites in the luxCDABE locus, which drives the expression of the bioluminescence genes, and two LuxR binding sites in the betIBA-proXWV promoter, which controls the expression of the osmotic stress response genes (van Kessel et al., 2015; Chaparian et al., 2016). The luxCDABE locus is one of the most highly activated by LuxR, and its expression is increased >100-fold in the presence of LuxR (van Kessel et al., 2013a; 2013b). Because few TetR-type proteins have been found to act as activators, the mechanism of activation and the reason that multiple binding sites are necessary for activation at this and other LuxR-regulated promoters remains unknown.

One proposed mechanism for LuxR transcription activation is that multiple binding sites enable LuxR interactions with other proteins. Importantly, two LuxR binding sites in the luxCDABE promoter in V. harveyi lie in close proximity to the –35 promoter recognition region of the promoter (Pribnow, 1975; Chaparian et al., 2016), suggesting that LuxR binding to these sites may facilitate an interaction with RNA polymerase (RNAP). In addition, we previously showed that LuxR DNA binding at yet another site in the luxCDABE promoter enables synergistic DNA binding with integration host factor (IHF), which drives proper timing of bioluminescence gene expression during quorum sensing (Chaparian et al., 2016). Related to this finding, IHF also plays a role in transcription activation of the vvpE promoter controlled by SmcR in V. vulnificus (Jeong et al., 2010). In this study by Jeong et al., IHF was shown to bind to two sites between the SmcR binding site and the –10/–35 in the vvpE promoter region. An in vivo assay demonstrated that the presence of IHF enabled co-immunoprecipitation of DNA bound by both RNAP and SmcR, whereas a strain lacking IHF did not immunoprecipitate both DNA fragments. From this experiment, the authors concluded that IHF bends the DNA to facilitate a direct interaction between SmcR and RNAP and that this interaction directs transcription activation. However, because this immunoprecipitation assay was performed in vivo, the proposed interaction between SmcR and RNAP may be direct or may be bridged by other proteins. Thus, these previous studies are suggestive of a role for LuxR-type proteins in interactions with RNAP to promote transcription activation, but none have conclusively demonstrated that this interaction directly occurs or whether it impacts transcription activation.

In this study, we demonstrate that LuxR directly interacts with RNAP both in vitro and in vivo in V. harveyi. Biochemical analyses show that LuxR interacts specifically with both the N-terminal and C-terminal domains of the α-subunit of RNAP in vitro. Mutations in specific interaction regions of LuxR decrease α-subunit binding affinity in vitro and abrogate transcription activation of quorum-sensing genes in vivo. Finally, we extend our findings to the closely related LuxR homolog HapR in V. cholerae and show that mutations in the analogous RNAP-interaction domain on HapR disrupt activation of quorum-sensing genes.

Results

LuxR interacts with RNAP in vivo

To identify potential proteins that interact with LuxR, an in vivo immunoprecipitation (IP) was performed using LuxR with a 1x-FLAG epitope tag (FLAG-LuxR) that has been shown to be fully functional in vivo (van Kessel et al., 2013b). Lysates from a V. harveyi ΔluxR strain containing FLAG-tagged LuxR (expressed via its native promoter on an extrachromosomal plasmid) or control strains were incubated with anti-FLAG beads, and proteins that remained bound to the beads through washing steps were analyzed by mass spectrometry (Fig. 1A and Tables S4–S6). The control strain tested was a ΔluxR strain containing an empty vector, and the empty vector control sample was also analyzed by mass spectrometry (Fig. 1A and Table S7). We also tested for proteins that interacted with the LuxR R17C mutant, which has been shown to be completely defective for DNA binding in vitro and in vivo (Fig. 1A) (Svenningsen et al., 2008, van Kessel et al., 2013b). Our analysis of proteins bound to anti-FLAG beads revealed numerous proteins (Fig. 1A), the majority of which were retained through high stringency buffer incubations (Fig. S1). LuxR was the most prominent band and several other expected proteins were also present (Fig. 1A). In addition, IHF was present in the list of proteins identified by mass spectrometry,

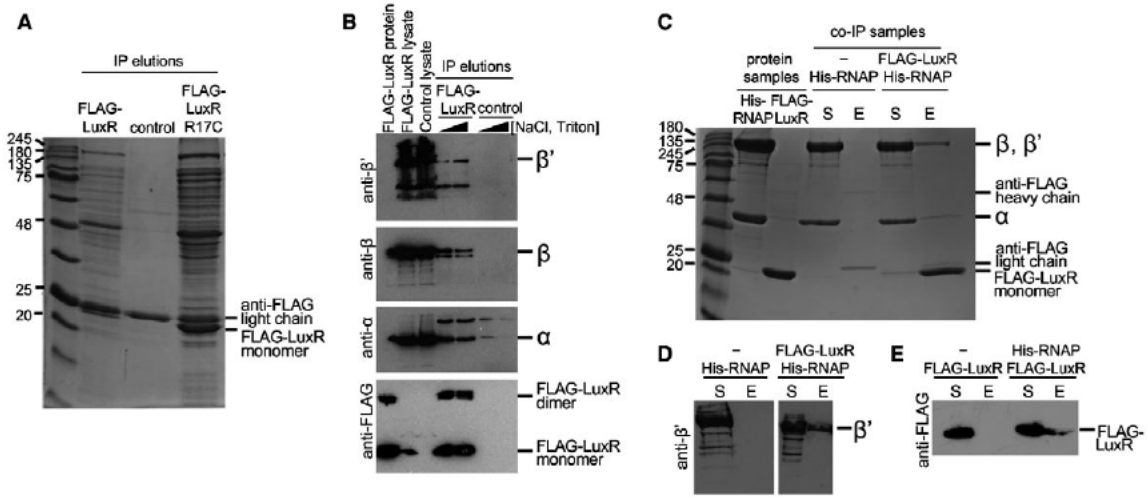

Fig. 1. LuxR interacts with RNAP in vivo and in vitro.

A. Elutions from IP reactions with a ΔluxR V. harveyi strain (KM669) containing plasmids expressing either FLAG-LuxR (pAP116), an empty vector control plasmid (pSLS3) or FLAG-R17C (pST012). The bands corresponding to the FLAG-LuxR protein and the light chain antibody to the FLAG epitope are indicated.

B. Western blot analyses of lysates and elutions from IP reactions with a ΔluxR V. harveyi strain (KM669) containing either a plasmid expressing FLAG-LuxR (pAP116) or an empty vector control plasmid (pSLS3). Purified FLAG-LuxR protein (1 μg) was included in lane 1 as a positive control for the FLAG western. For each strain, two IP reactions were tested with differing stringencies in the wash steps: (i) 100 mM NaCl, 0.1% Triton-X and (ii) 500 mM NaCl, 1% Triton-X. Antibodies used are indicated on the left of each panel.

C, D. SDS-PAGE (C) and western blot (D) analyses of co-IP experiments with purified FLAG-LuxR and His-RNAP holoenzyme incubated with anti-FLAG resin. Purified E. coli His-RNAP (216 pmol) and purified FLAG-LuxR (54 pmol) were loaded in lanes 2 and 3, respectively, in panel C. Samples were taken of the supernatants (S) after incubation with the anti-FLAG resin and samples of the elution (E) were collected from the resin after elution. The western blot was probed with antibodies against β′.

E. Western blot analysis of reciprocal co-IP experiments performed with FLAG-LuxR and His-RNAP incubated with nickel-NTA resin. Samples were taken of the supernatants (S) after incubation with the nickel-NTA resin and samples of the elution (E) were collected from the resin after elution. The western blot was probed with antibodies against the FLAG epitope.

which has been previously shown to interact with LuxR in vitro (Chaparian et al., 2016). Catabolite activator protein (CAP) was also identified, which is required for transcription activation at some LuxR-activated promoters (Chatterjee et al., 2002). We observed that some of the most prominent proteins in the LuxR IP were subunits of RNAP. We identified the core enzyme subunits α, β, and β′, as well as several sigma factors (σ^{70}, σ^{38}, σ^{54}; Tables S4–S6). Importantly, RNAP holoenzyme proteins were also identified in IPs performed with the DNA-binding mutant FLAG-LuxR R17C (Fig. 1A; data not shown). In IPs with the FLAG-LuxR R17C mutant protein, the LuxR band is more prevalent because LuxR autorepresses its expression (Chatterjee et al., 1996). Thus, the DNA-binding mutant cannot bind DNA to repress its own expression and FLAG-LuxR R17C has higher levels of LuxR expression and immunoprecipitates more proteins. The R17C DNA binding mutant shows that the proteins are being pulled down by a LuxR-protein interaction and not simply by LuxR binding DNA and pulling down proteins that are also bound to that segment of DNA. The results of these experiments suggested that LuxR interacts with RNAP in vivo, and this interaction is independent of DNA binding by LuxR. To corroborate the mass spectrometry results, western blot analyses were performed with antibodies against RNAP α, β and β′. These RNAP subunits were observed in IP elutions only in the strain containing FLAG-LuxR and not in a control strain (Fig. 1B). Thus, we conclude that LuxR interacts with RNAP in vivo in V. harveyi.

LuxR directly interacts with RNAP in vitro

To test if LuxR and RNAP directly interact, both proteins were purified and a co-immunoprecipitation (co-IP) experiment was performed. V. harveyi FLAG-LuxR was the bait protein to test whether it could pull down E. coli His-RNAP using anti-FLAG beads. We chose to use purified E. coli RNAP for these assays for three reasons: (i) we have shown that LuxR-activated genes (e.g. luxCDABE) are expressed in E. coli in the presence of LuxR (van Kessel et al., 2013b), (ii) V. harveyi RNAP subunits share 82–91% amino acid identity with E. coli RNAP subunits, and (iii) expression plasmids for E. coli RNAP purification were readily available. Following the co-IP, His-RNAP was observed to only be present in the elutions of reactions that also contained FLAG-LuxR (Fig. 1C), and this result was confirmed by western blot

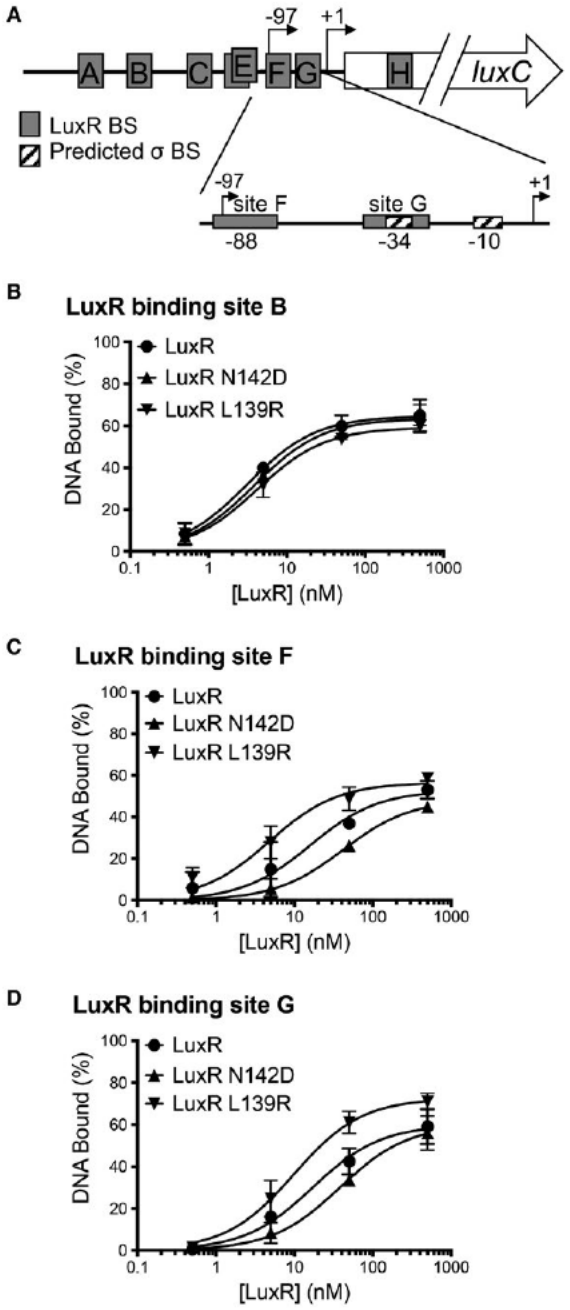

Fig. 2. LuxR DNA binding to P_{luxC} promoter binding sites.
A. Diagram of the luxCDABE promoter region. Gray boxes indicate LuxR binding sites (BS) and hatched boxes are predicted σ BSs. The primary transcription start site is indicated by a black arrow at +1, and the upstream low cell density transcription start site is indicated by a black arrow at –97.
B, C, D. Electrophoretic mobility shift assays were conducted with dsDNA substrates corresponding to LuxR binding sites B (panel B; oligos JCV617, JCV363), F (panel C; oligos AB190, AB191) or G (panel D; oligos AB188, AB189) with purified proteins LuxR, LuxR N142D and LuxR L139R at concentrations ranging from 0.5 to 500 nM. The percentage of DNA bound is graphed for each protein. A two-way analysis of variance (ANOVA) followed by Tukey's multiple comparison test (n = 3) was performed on all data points, and no statistical differences were observed ($p < 0.001$).

analysis (Fig. 1D). Reciprocal reactions were performed in which His-RNAP acted as the bait protein using nickel-NTA resin. FLAG-LuxR was only observed to be present in the elutions of the reactions that also contained His-RNAP (Fig. 1E). These results show that LuxR directly interacts with RNAP in vitro.

LuxR binds to two sites proximal to the –10/–35 region of the luxCDABE promoter

To determine whether LuxR interactions with RNAP are relevant to LuxR activity as a transcriptional regulator in V. harveyi, we examined promoters in which LuxR binds proximally to RNAP. Although LuxR binding site locations in the V. harveyi genome have been determined by ChIP-seq (van Kessel et al., 2013b), transcription start sites are not known for most promoters in V. harveyi. Thus, LuxR binding site positions relative to transcription start sites are not known for most genes. However, previous work has identified many LuxR binding sites in the promoter of the luxCDABE operon, two of which that lie in close proximity to the defined primary transcription initiation site (Fig. 2A) (Chaparian et al., 2016). There are two known transcription start sites at this promoter; the upstream low cell density start site (Fig. 2A, labeled at –97) is weak and repressed by LuxR, and the downstream high cell density start site (Fig. 2A, labeled at +1) is the primary site for high levels of transcription initiation during quorum sensing (Swartzman et al., 1992; Swartzman and Meighen, 1993). LuxR binding sites A-G are all necessary for transcription activation at the primary start site to varying degrees; scrambling the LuxR-binding sequence at these binding sites eliminates expression of the luxCDABE genes (Chaparian et al., 2016). Specifically, site F is centered at –88 upstream of the primary transcription start site, and site G is centered at –34, directly over the predicted –35 site. Because the F and G LuxR binding sites are both candidates for LuxR positioning near RNAP for interaction at this promoter, we examined the binding affinity for LuxR at these sites relative to a site distantly located from the transcription start site (site B). Site B is a highly studied binding site for LuxR at this promoter, and LuxR is known to have a high affinity to site B (van Kessel et al., 2013b). Thus, we wanted to compare LuxR binding at site B with the relatively newly discovered LuxR binding sites F and G. Electrophoretic mobility shift assays (EMSAs) were performed with LuxR and DNA containing sites B, F or G from the luxCDABE promoter (Fig. 2 and Fig. S2). The binding affinity for LuxR to site B was relatively high at 3.2 nM and is similar to previously published results (Fig. 2B and Fig. S2A; previously calculated at 14.7 nM [van Kessel et al., 2013b]). We calculated the binding affinity for LuxR to sites F and

G to be 16.0 and 17.1 nM respectively (Figs 2C,D, S2B and S2C). Thus, the binding affinities for sites F and G are in a similar range as site B (van Kessel et al., 2013b). We conclude that LuxR binds with specificity to sites F and G that are in close proximity to RNAP during transcription initiation at the luxCDABE promoter.

LuxR directly interacts with the RNAP α-subunit N- and C-termini

To identify which subunit of RNAP interacts with LuxR, E. coli His-α was purified (Tang et al., 1995). The α-subunit was chosen first for these experiments for two reasons: (i) It is the only subunit that can fold correctly in the absence of the other RNAP core enzyme subunits and can therefore be purified in the absence of the other subunits (Tang et al., 1995) and (ii) many activator proteins that are known to interact with RNAP, such as Fis and CAP, have been shown to interact with the α-subunit (Heyduk and Heyduk, 1993; Bokal et al., 1995). Co-IP experiments were performed with FLAG-LuxR and His-α. Using FLAG-LuxR as the bait, the α-subunit was found to only be present in the reactions containing FLAG-LuxR (Fig. 3A). From these data, we conclude that LuxR directly interacts with the α-subunit. However, this finding does not rule out the possibility of additional interactions with other subunits of RNAP.

Several specific interaction interfaces have been identified on the α-subunit of RNAP (Savery et al., 2002). Most proteins interact with the C-terminus of α (Bell et al., 1990; Igarashi et al., 1991; Ishihama, 1992; Niu et al., 1996), though CAP is known to interact with both the N-terminal domain (NTD) and C-terminal domain (CTD) of α at class II promoters (Niu et al., 1996). To further assess the interaction between LuxR and the α-subunit, we used Bio-layer interferometry (BLI) to measure the relative dissociation constant (K_d) between these proteins in an in vitro assay. In this assay, one protein, the 'ligand', is immobilized on a biosensor tip and incubated with various concentrations of a second protein, the 'analyte'. The purpose of this assay is to provide a relative quantitative measurement to compare proteins in vitro, but is not intended to indicate the in vivo binding affinity between proteins. In our initial experiments, E. coli His-α was used as the ligand and immobilized with Ni-NTA biosensor tips, and native LuxR served as the analyte. The K_d between LuxR and His-α was determined to be 150 nM (Fig. 3B and Table 1). We next purified two mutant versions of the His-α protein: ΔCTD and ΔNTD. When we performed a BLI experiment with LuxR and His-α ΔCTD, we found the K_d to be 256 nM, which is statistically different ($p = 0.007$) than the K_d between LuxR and His-α (Fig. 3C and Table 1). Unfortunately, the ΔNTD protein did not stably associate with the BLI sensor tip, and thus the BLI experiment could not be performed with this mutant protein (data not shown). Our result with the ΔCTD protein suggests that the N-terminal domain of α is not sufficient for maximal interaction with LuxR. However, because there was still a definite observed interaction between LuxR and His-α ΔCTD with a moderate affinity, we conclude that there are binding interaction sites between LuxR and the NTD of α. As a negative control for this experiment, we performed BLI with purified His-tagged Tobacco Etch Virus Nla proteinase (His-TEV protease) as the ligand and LuxR as the analyte (Blommel and Fox, 2007). Because the mass spectrometry data from the LuxR IP experiment indicated that LuxR has the ability to interact with many proteins in vivo, we chose to test a negative control protein for its ability to interact with LuxR in the BLI assay. We chose His-TEV protease because (i) we had an active batch of TEV protein purified, (ii) it is a protein that is not natively expressed in V. harveyi and (iii) our preparation contained a His-tag for use in western blots and BLI experiments. Neither an association nor a dissociation were observed for experiments with His-TEV and LuxR, and a K_d could not be calculated (Fig. 3D and Table 1). Thus, we conclude that LuxR specifically interacts with the α-subunit of RNAP in vitro and the N-terminal domain of α contributes to some, but not all, of this interaction, requiring the C-terminal domain for maximal interaction. In addition, we purified the α-subunit of RNAP from V. harveyi and determined that it has a K_d of 139 nM for binding to LuxR, which is not significantly different from the binding affinity of LuxR to E. coli α (Fig. 3E and Table 1, $p = 0.999$).

Identification of the interaction interface on LuxR that interacts with the RNAP α-subunit

Though we demonstrated that the LuxR-α interaction is mediated through both the NTD and CTD of α,it was unknown where the interaction occurs on the LuxR dimer. To identify LuxR amino acids in the interface of the LuxR-α interaction, we developed a peptide array assay to probe the LuxR protein sequence. A synthetic peptide array of the LuxR protein primary structure was synthesized using 10 amino acid peptides spotted on a membrane, with 7 amino acid overlaps in sequence between neighboring peptides (Fig. 4A and Fig. S3A). We incubated this peptide membrane with purified E. coli His-RNAP and probed for RNAP using an anti-β′ antibody. Spots on the array clearly identified where His-RNAP interacted with LuxR peptides (Fig. 4B). We mapped these onto the crystal structure of the LuxR homolog SmcR to visualize the relative arrangement of these peptides near the DNA-binding domain (helices 2 and 3), dimerization domain (helices 8 and 9)

and the ligand-binding pocket (helices 4–8) (Fig. 4E) (Kim et al., 2010; 2018). We observed that RNAP interacts with peptides corresponding to alpha helices 1, 4 and 7, as well as an N-terminal region near (but not part of) the helices in the DNA-binding domain (Fig. 4E). None of the peptide hits were in the dimerization domain. Among the peptides that interact with RNAP are two residues that were previously studied: L139 and N142. Substitutions at these LuxR residues (L139P, L139R and N142D) result in a LuxR activation defect in which multiple promoters (including luxCDABE) have decreased or no transcription activation, with no apparent effect on LuxR repression at any tested promoter (van Kessel et al., 2013b).

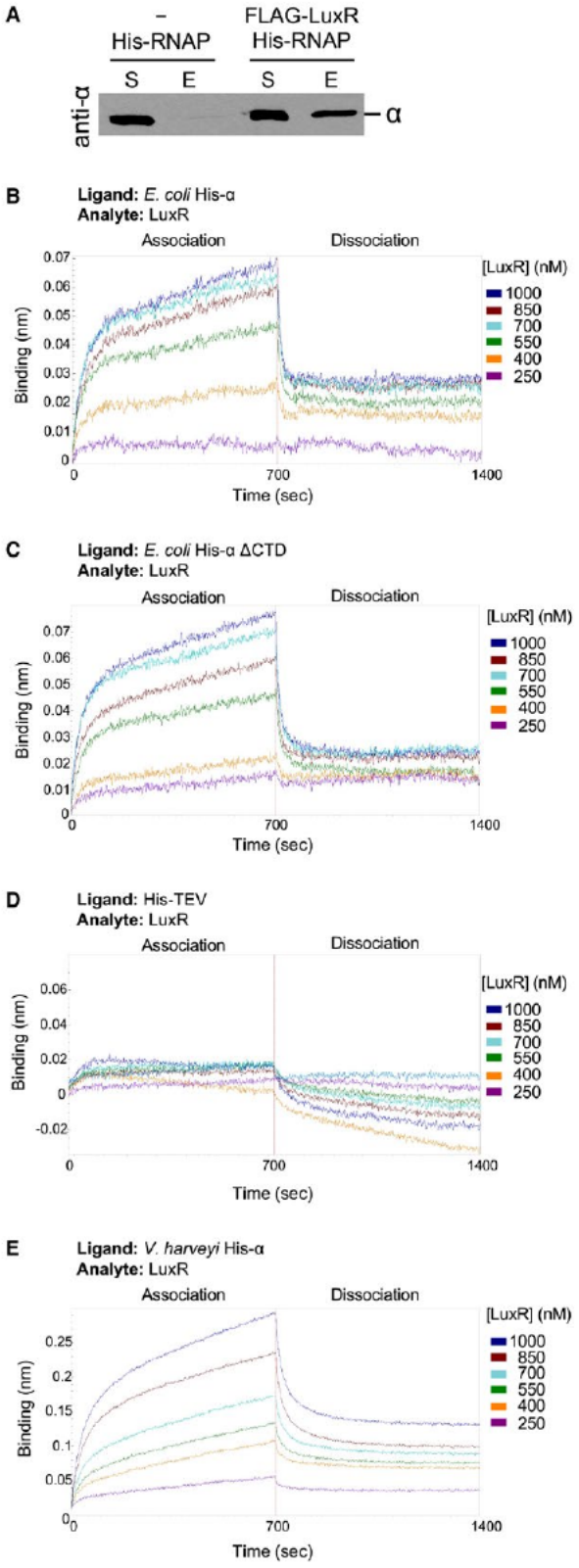

Fig. 3. LuxR interacts with the N-terminal domain of RNAP α subunit.
A. Western blot analysis of co-IP experiments with purified FLAG-LuxR and E. coli His-α incubated with anti-FLAG resin. Samples were taken of the supernatants (S) after incubation with the anti-FLAG resin and samples of the elution (E) were collected from the resin after elution. The western blot was probed with antibodies against α.
B, C, D, E. BLI analyses of LuxR (analyte) interactions with various ligands (each at 200 nM): E. coli His-α (B), E. coli His-α ΔCTD (C), His-TEV protease (D) or V. harveyi His-α (E). LuxR concentrations are indicated, and the association and dissociation curves are presented. [Colour figure can be viewed at wileyonlinelibrary.com]

We also probed the LuxR peptide array with V. harveyi RNAP subunit α (Fig. 4C). We observed that the α subunit binds a specific subset of the regions of LuxR that the RNAP holoenzyme was found to bind: helices 1, 4 and 7. As a negative control, we probed the LuxR peptide array with His-TEV protease (Fig. 4D). The purpose of this control was to identify non-specific 'sticky' regions of the LuxR peptide array and differentiate specific regions of LuxR required for protein-protein interactions. Only three spots had a strong signal on this control peptide array with His-TEV protease. This result demonstrates that only a single region of LuxR on alpha helix 4 is a 'sticky' area that enabled binding of all three proteins tested in this assay, though this region may still be important for LuxR-protein interactions. We conclude that RNAP holoenzyme and RNAP α bind to specific regions of LuxR in helices 1, 4 and 7 and in the unstructured N-terminus.

Mutations in the LuxR interaction interface disrupt the LuxR-α interaction

Because RNAP interacts with peptides from multiple regions of LuxR, we used a genetic approach to determine the key residues required for the LuxR-α interaction from among those identified in the peptide array. We made alanine substitutions in various amino acid residues that were prevalent in the peptides bound by RNAP in the peptide array, specifically in the N-terminal loop and helices 4 and 7 (Fig. 4E). Using a previously established assay in E. coli (van Kessel et al., 2013b), we measured transcription activation and repression driven

by expression of luxR mutant alleles using fluorescent reporters: activation is measured using a $P_{luxCDABE}$-gfp reporter and repression is measured using a P_{05222}-mCherry reporter. For example, wild-type LuxR activates transcription of $P_{luxCDABE}$ (high GFP levels) and represses transcription of P_{05222} (low mCherry levels) compared to the empty vector control strain (Fig. 4F). Conversely, a DNA-binding defective LuxR R17C mutant does not activate transcription of $P_{luxCDABE}$ (low GFP levels) and does not repress transcription of P_{05222} (high mCherry levels) (Fig. 4F). As shown previously, L139P, L139R and N142D have wild-type levels of repression but have major activation defects (Fig. 4F). We also observed activation-defective phenotypes in most of the tested LuxR mutant proteins, such as for R73A and S76A (Fig. 4F). To test whether mutations in different helices had combinatorial effects in this assay, we constructed double mutant alleles. The phenotype of a strain expressing a LuxR allele with a combination of the L139P and N142D mutations was not additive (Fig. S3B), nor was combination of the N142D and S76A mutations (Fig. S3C), suggesting that the activation defect for each mutant allele is likely linked to the same interaction interface. We also observed some mutant proteins that have an increased activation phenotype (P8A, Q141A and N142I).

To further assess the phenotypes of the luxR mutants identified in the E. coli reporter screen, we constructed V. harveyi ΔluxR strains containing wild-type or mutant luxR alleles expressed by induction on extrachromosomal plasmids and assayed for activation of the

Table 1. BLI analyses of LuxR-protein interactions.

Ligand[a]	Analyte[a]	K_d (nM)	R^2
His-α E. coli	LuxR	150 ± 3	0.891
His-α ΔCTD E. coli*	LuxR	255 ± 37	0.922
His-α V. harveyi	LuxR	139 ± 19	0.898
His-TEV protease	LuxR	ND	ND
His-α V. harveyi	LuxR N142D*	376 ± 24	0.901
His-α V. harveyi	LuxR L139R	128 ± 17	0.981
His-α V. harveyi	LuxR S76A*	250 ± 51	0.997
His-α V. harveyi	LuxR I4A	198 ± 24	0.970
His-α V. harveyi	LuxR S76A/N142D*	327 ± 36	0.964

[a]An * indicates that the mutant protein is significantly different than the wild-type protein counterpart ($p < 0.01$; one-way analysis of variance (ANOVA), followed by Tukey's multiple comparison test; n = 3).

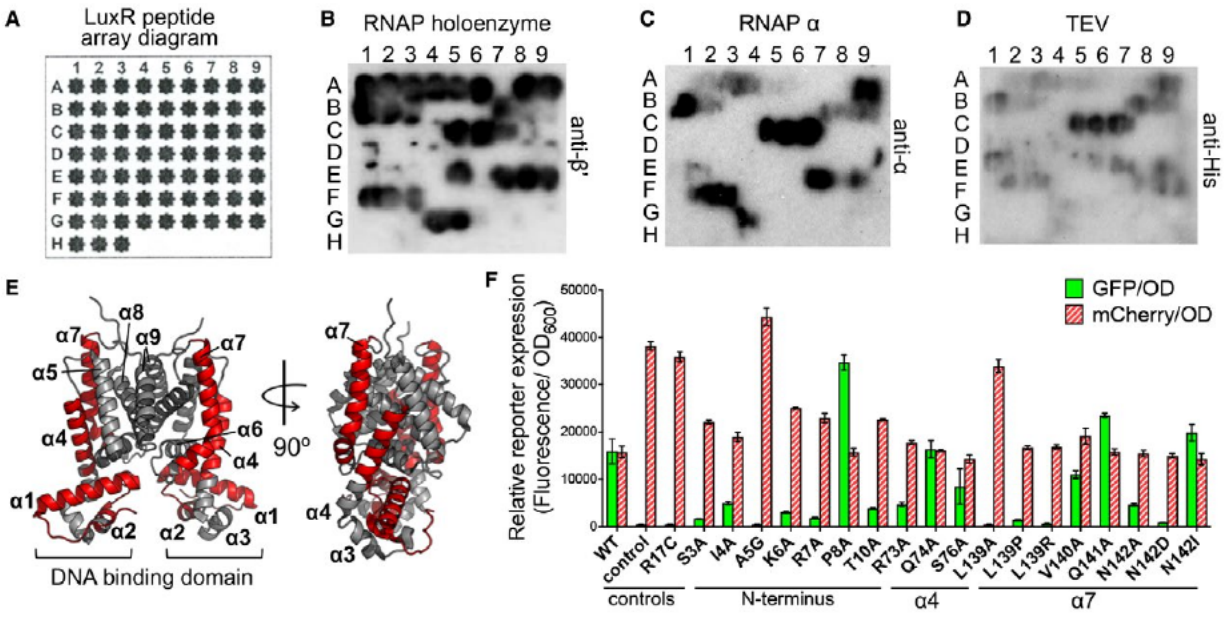

Fig. 4. The LuxR-RNAP interaction domain on LuxR revealed by peptide arrays and in vivo assays.
A. Diagram of LuxR peptide array layout; corresponding peptides presented in Figure S2A. B, C, D. LuxR peptide array probed with His-RNAP (panel B, western blot against β′), E. coli His-α (panel C, western blot against α) or His-TEV protease (panel D, western blot against 6xHis epitope). E. Crystal structure of V. vulnificus SmcR (PDB: 3KZ9, gray); image generated by PyMol. The LuxR peptides identified in the peptide array that interact with RNAP are highlighted in red. F. GFP and mCherry expression from E. coli strains containing plasmids expressing LuxR (pJV239), LuxR R17C (pAB38), empty vector (pJV036) or LuxR with amino acid substitutions as listed (see Table S2 for all plasmid names). Relative fluorescence expression was calculated by dividing the fluorescence value by the OD_{600} value. The locations of amino acid substitutions in LuxR are indicated (N-terminus, α-helix 4 or α-helix 7). [Colour figure can be viewed at wileyonlinelibrary.com]

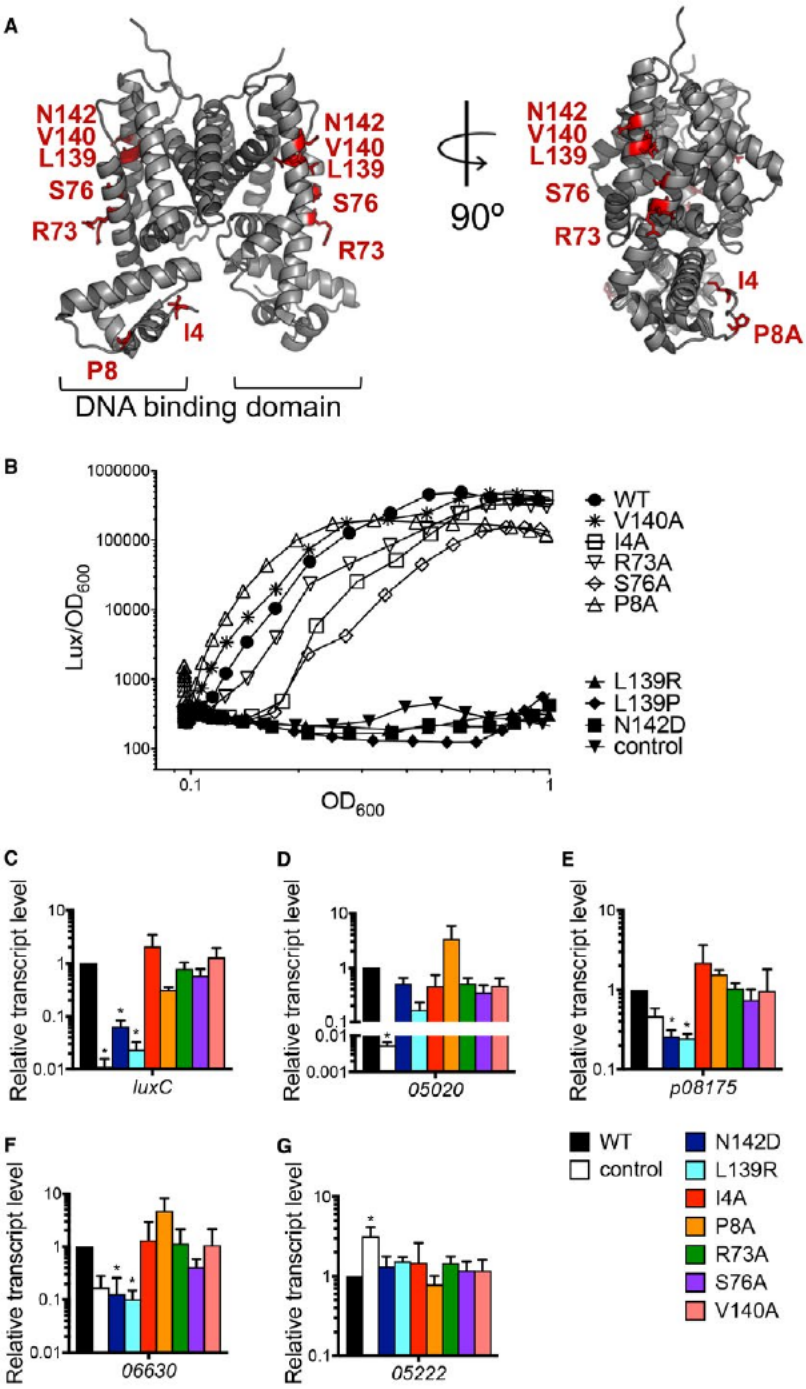

Fig. 5. Amino acid substitutions in the RNAP interaction domain on LuxR alter gene expression.
A. Crystal structure of V. vulnificus SmcR (PDB: 3KZ9, gray); image generated by PyMol. The amino acids for which substitutions are assayed in panel B are indicated by red sticks.
B. Bioluminescence assay with V. harveyi ΔluxR strains (KM699) containing plasmids expressing wild-type LuxR (WT; pJV239), empty vector (control; pJV036), LuxR N142D (pJV261), LuxR L139R (pJV260), LuxR L139P (pJV242), LuxR I4A (pAB17), LuxR P8A (pAB21), LuxR R73A (pAB25), LuxR S76A (pAB28) or LuxR V140A (pAB33). Bioluminescence is calculated as light units (lux) per OD_{600}. Data points represent mean values for three independent experiments.
C, D, E, F, G. Relative transcript levels of V. harveyi genes were determined by qRT-PCR from the same V. harveyi ΔluxR strains and plasmids expressing LuxR alleles as described in panel B for genes luxC (C), VIBHAR_05020 (D), VIBHAR_p08175 (E), VIBHAR_06630 (F) and VIBHAR_05222 (G). The legend for panels C–G denotes the LuxR allele expressed on a plasmid for each strain. Asterisks indicate significant differences compared to the WT luxR phenotype ((C, D): $p < 0.0001$; one-way ANOVA, followed by Tukey's multiple comparisons test of log-transformed data; n = 3); (E): $p < 0.05$; one-way ANOVA, followed by Dunnett's multiple comparisons test; n = 3); (F,G): $p < 0.05$; one-way ANOVA, followed by Dunnett's multiple comparisons test of log-transformed data; n = 3). [Colour figure can be viewed at wileyonlinelibrary.com]

luxCDABE promoter by LuxR and mutant LuxR proteins. Because we used an IPTG-inducible promoter, LuxR production was not regulated by quorum sensing but rather by addition of IPTG. Thus, we performed a bioluminescence time course to observe LuxR regulation of bioluminescence following induction. We chose to focus on eight mutants with the most dramatic activation-specific phenotypes in the E. coli assay and mapped these onto the SmcR crystal structure (Fig. 5A): I4A, P8A, R73A, S76A, V140A, L139P, L139R and N142D (van Kessel et al., 2013b). The mutants were determined to have activation-specific phenotypes if they retained WT levels of repression. All of the mutants but LuxR P8A and V140A had a decreased and/or delayed bioluminescence phenotype (Fig. 5B). The L139P, L139R and N142D luxR mutations completely abrogated bioluminescence activation and were comparable to the empty vector control strain (Fig. 5B). LuxR S76A displayed a delayed onset of bioluminescence as well as lower levels of bioluminescence throughout the curve. LuxR P8A had an accelerated onset of bioluminescence but ultimately failed to reach WT levels of bioluminescence. LuxR V140A behaved similarly to wild-type LuxR and did not show a phenotype in this assay. Western blot analysis showed that all LuxR proteins were produced at similar levels, indicating that phenotypic differences were not due to protein level (Fig. S4).

We also analyzed expression of several quorum-sensing genes that are directly activated by LuxR: luxC, VIBHAR_05020, VIBHAR_p08175 and VIBHAR_06630. Our qRT-PCR analyses comparing strains expressing wild-type LuxR versus mutant LuxR show that the LuxR N142D and L139R alleles were significantly decreased in activation at all tested LuxR-activated promoters except VIBHAR_05020 (Fig. 5C–F). As we observed with the bioluminescence data, L139P and L139R have the same phenotype (Fig. 5B, data not shown). Conversely, strains expressing the LuxR I4A, P8A, R73A and V140A mutant proteins had varied phenotypes at activated promoters with differing levels of activation but none were significantly different from wild-type LuxR (Fig. 5C–F). All mutant proteins displayed wild-type levels of repression at VIBHAR_05222, a repressed gene in the LuxR regulon (Fig. 5G) (van Kessel et al., 2013a; 2013b). These results suggest that the N142D, L139P and L139R mutations disrupt the interaction between LuxR and RNAP at most activated promoters. However, the variable phenotypes of the other mutant alleles suggest that there may be other effects of these mutations at each promoter.

We next assayed the effects of LuxR amino acid substitutions on the interaction between LuxR and V. harveyi α in vitro using BLI. Surprisingly, we observed that the K_d between LuxR L139R and His-α was not significantly different from the K_d between wild-type LuxR and His-α (128 and 139 nM respectively), suggesting that this substitution alone does not disrupt the interaction measured in vitro (Table 1 and Fig. S5A). Conversely, the K_d between LuxR N142D and His-α was calculated to be 376 nM, which is a significant 2.7-fold decrease in binding affinity compared to wild-type LuxR (Table 1 and Fig. S5B). We assayed the DNA binding affinity of LuxR mutant proteins L139R and N142D to LuxR binding sites F and G from the luxCDABE promoter. The binding affinities for LuxR L139R at sites B, F and G were similar to wild-type LuxR and not significantly different at any point assayed (Fig. 2B–D, 4.2, 4.8, and 9.5 nM, respectively; $p < 0.001$). The binding affinities for LuxR N142D at sites B, F, and G were also similar to wild-type LuxR and not significantly different (Fig. 2B–D, 3.9, 41.9 and 38.1 nM, respectively; $p < 0.001$). From these results, we conclude that the L139R and N142D substitutions do not affect DNA binding at any site proximal to RNAP. The N142D substitution causes a decrease in interaction with RNAP α, which likely results in the observed defects in transcription activation in vivo.

BLI experiments were also performed with LuxR mutant proteins I4A and S76A because the strains containing these mutant alleles displayed a decrease in activation at several promoters (Fig 5B,C). The K_d between V. harveyi His-α and LuxR I4A or LuxR S76A was calculated to be 198 and 250 nM respectively (Table 1 and Fig. S5C,D). Although LuxR I4A appears to have a slight binding defect compared to wild-type LuxR binding with the α subunit (139 nM), it is not significant ($p = 0.222$). However, LuxR S76A has a significant 1.8-fold decrease ($p = 0.005$) in binding affinity compared to wild-type LuxR (Table 1 and Fig. S5D). This indicates that the activation deficiency displayed by LuxR S76A is likely due to a decrease in binding with RNAP α.

Mutation of the RNAP α interaction domain of HapR disrupts transcription activation in V. cholerae

LuxR homologs in Vibrio species share high percent identities, particularly in the DNA-binding domain (van Kessel et al., 2013b). However, the amino acid identity is less well-conserved in the region near alpha helices 4–7 (Fig. 6A). We examined the conservation of amino acid residues at the key LuxR interaction positions identified by our in vitro experiments and observed that these residues are highly conserved between LuxR, SmcR, HapR and OpaR. Conversely, these residues are strikingly absent in the alignment with E. coli TetR. In addition, LitR has no identity with LuxR at these residues, though LitR encodes amino acids that may have functional conservation (e.g. valine at position 139 in place of the leucine in LuxR, or histidine in position 76 in place of the serine in LuxR). Given the high identity between LuxR proteins in these Vibrio species,

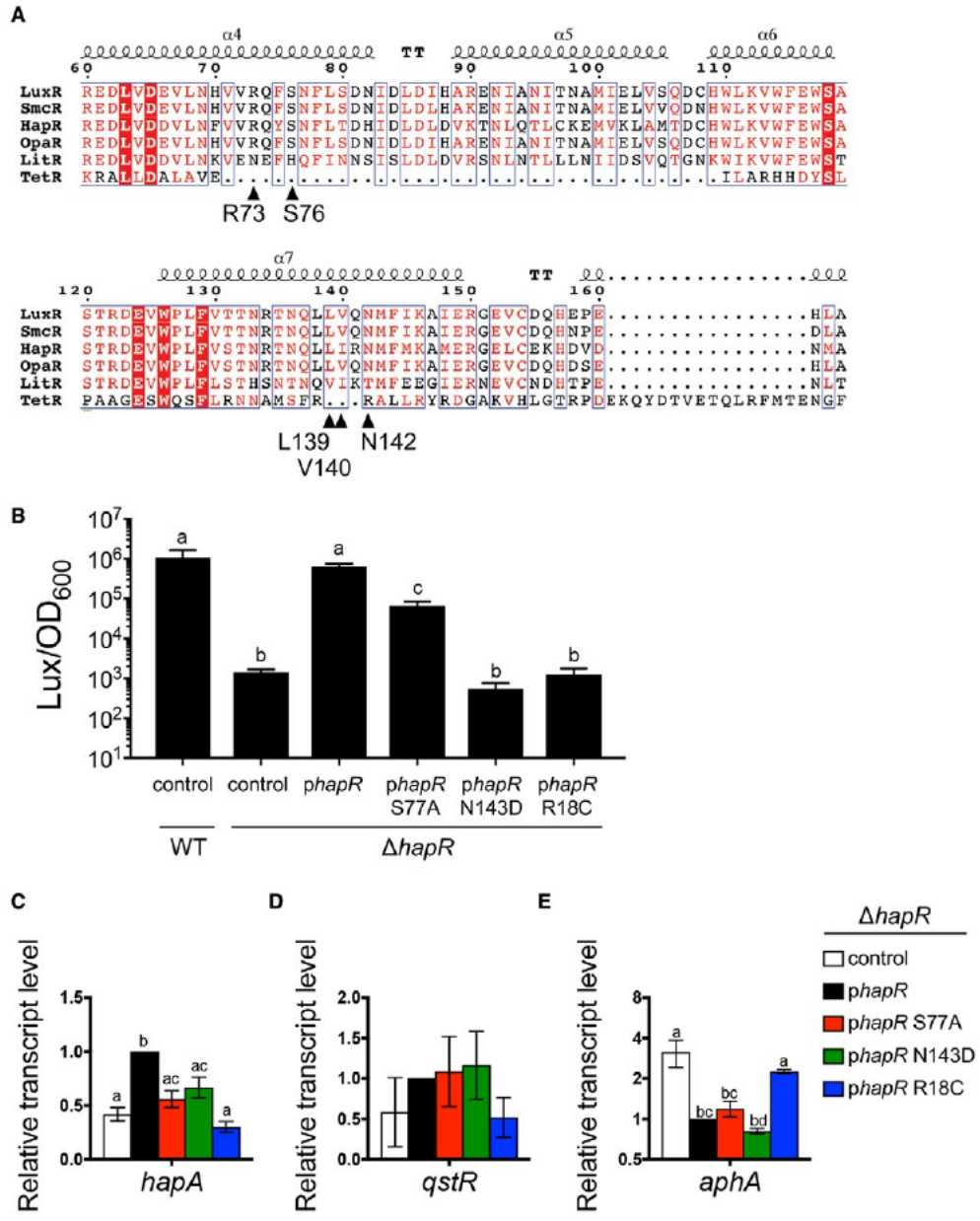

Fig. 6. Amino acid substitutions in HapR alter gene expression.
A. Alignment of predicted RNAP interaction domains of LuxR homologs from V. harveyi (LuxR, AAA27539), V. vulnificus (SmcR, AAF72582), V. cholerae (HapR; ABD24298), V. parahaemolyticus (OpaR, NP_798895) and V. fischeri (LitR, YP_205560) aligned to E. coli TetR (P0ACT4). Sequence alignments were assembled using the Clustal Omega software program (Sievers et al., 2011) and viewed using the ESPript program (Robert and Gouet, 2014). Black triangles indicate the location of amino acids shown. The predicted alpha helices are shown above the alignment.
B. Endpoint bioluminescence assay with V. cholerae wild-type and ΔhapR strains (AC53 and SAD793 respectively) containing plasmids expressing wild-type hapR (WT; pSLS1096), empty vector (control; pEVS143), hapR S77A (pJV377), hapR N143D (pJV378) or hapR R18C (pJV379). Bioluminescence is calculated as light units per OD_{600} (relative light units, RLU). Different letters indicate significant differences ($p < 0.0001$; one-way ANOVA, followed by Tukey's multiple comparisons test of log-transformed data; n = 3).
C, D, E. Relative transcript levels of V. cholerae genes were determined by qRT-PCR from V. cholerae ΔhapR strains containing plasmids expressing hapR (pSLS1096), empty vector (control; pEVS143), hapR S77A (pJV377), hapR N143D (pJV378) or hapR R18C (pJV379). Different letters indicate significant differences ($p < 0.05$; one-way ANOVA, followed by Dunnett's multiple comparisons test (C) or Tukey's multiple comparisons test (D, E) of log2-transformed data; n = 3). [Colour figure can be viewed at wileyonlinelibrary.com]

we hypothesized that these residues are important for RNAP interactions in these species as well. To test this, we examined the effects of making substitutions in V. cholerae HapR in the residues analogous to LuxR N142 and S76 (which correspond to N143 and S77 in HapR respectively). We also constructed the analogous R17C

DNA-binding deficient substitution in HapR (which corresponds to R18C in HapR). The hapR wild-type and mutant alleles were cloned onto extrachromosomal plasmids under control of the IPTG-inducible P_{tac} promoter in a ΔhapR V. cholerae strain background and compared to a wild-type V. cholerae strain. We first tested the bioluminescence phenotype of strains expressing these mutant proteins using a low-copy plasmid containing the luxCDABE locus (operon and native promoter) from V. harveyi. This experiment with hapR alleles was performed with 1 μM IPTG, which produced comparable levels of bioluminescence in a ΔhapR strain containing the hapR expression plasmid compared to the wild-type strain (Fig. 6B).

Bioluminescence production exhibited significant decreases of 10-fold and 1177-fold in strains expressing hapR S77A and N143D, respectively, compared to the strain expressing wild-type hapR (Fig. 6B). As expected, bioluminescence production was completely abrogated in the strain expressing the hapR R18C DNA-binding mutant. Interestingly, the defective phenotypes of hapR N143D and S77A were restored to wild-type bioluminescence levels upon overexpression with 10 μM IPTG, whereas the R18C mutant was not changed (Fig. S6). From these results, we conclude that the N143D and S77A HapR residues are required for maximal expression of the luxCDABE genes in V. cholerae under conditions of endogenous hapR levels. Because these substitutions in HapR result in similar phenotypes to the analogous substitutions in the RNA polymerase interaction domain of LuxR, the data suggest that HapR interacts with RNA polymerase via the same interaction domain on HapR as on LuxR.

We next assayed transcript levels of quorum-sensing genes in V. cholerae that have previously been shown to be directly activated by HapR: hapA and qstR (Jobling and Holmes, 1997; Tsou et al., 2009; Zheng et al., 2011; Lo Scrudato and Blokesch, 2013; Metzger et al., 2016). As a control for HapR transcription repression activity, we assayed transcript levels of aphA. As expected, only the hapR R18C DNA-binding mutant was unable to repress, indicating there is no defect in the DNA binding ability of hapR S77A and N143D. In strains containing the hapR S77A and N143D mutants, transcript levels significantly decreased ~2 fold for hapA compared to wild-type hapR (Fig. 6C). Conversely, none of the mutants exhibited significant differences in qstR transcript levels compared to wild-type hapR (Fig. 6D). This is a similar finding to our results in V. harveyi where some, but not all, LuxR-activated genes were affected by the S76A and N142D substitutions. From these qRT-PCR and bioluminescence data, we conclude that substitutions in HapR N143D and S77A decrease transcription at specific promoters in V. cholerae. This suggests that the RNAP interaction domain is conserved in HapR.

Discussion

At tightly controlled promoters with suboptimal sigma factor binding site consensus sequences, activators are often required to recruit, stabilize or aid in open complex formation during transcription activation. In this study, we identified the interaction between the V. harveyi master regulator, LuxR and RNAP. We found that LuxR and RNAP directly interact, and this interaction is likely necessary for the proper expression of some quorum sensing-regulated genes. LuxR interacts with RNAP at both the NTD and CTD of the α subunit, though our data have not ruled out the possibility that LuxR may also interact with other subunits of RNAP holoenzyme. The likelihood that LuxR interacts with other subunits of RNAP is supported by the results of our experiments with LuxR peptide arrays. Both the RNAP holoenzyme and the α subunit alone interacted with sites on the peptide array with the majority of these sites overlapping. However, the RNAP holoenzyme displayed more interaction sites on LuxR peptides than α alone. These extra interaction sites between RNAP and LuxR could be mediated by the other subunits of RNAP. The interaction between LuxR and the α-NTD is especially interesting because few proteins, such as CAP, have been shown to interact in that region of the α subunit (Niu et al., 1996; Rhodius et al., 1997; Lee et al., 2012). It is likely that both α-CTD and α-NTD interactions are required at LuxR binding sites that overlap the –35, as both are required at similar CAP class II promoters.

Another important similarity to note between LuxR and CAP is that CAP is capable of binding to promoters in almost exactly the same positions relative to RNAP as LuxR does at $P_{luxCDABE}$ in V. harveyi. At class I CAP-activated promoters, CAP binds at a site centered at –62 to –103 bp upstream of the transcription start site and interacts with the α-CTD, while at class II CAP activated promoters, CAP binds to a site centered at –41bp that overlaps with the –35 element and replaces it while it interacts with the α-CTD, α-NTD and σ^{70} (Gaston et al., 1990; Niu et al., 1994; 1996; Zhou et al., 1994a; 1994b; Rhodius et al., 1997; Savery et al., 1998; Rhodius and Busby, 2000a; 2000b). At $P_{luxCDABE}$, LuxR binds to a site centered at –88 (site F) and a site centered at –34 (site G), and we have also shown an interaction between LuxR and the α-NTD and α-CTD. Another TetR-type protein, DhaS in Lactococcus lactis, had been found to be an activator instead of a canonical TetR repressor. DhaS has been found to interact with another protein, DhaQ, to activate the dha operon. Not only was this TetR-type protein found to interact with another protein, like LuxR, but it also has a binding site in the promoter of the dha operon that overlaps with the –35 binding site of RNAP (Christen et al., 2006). This information, coupled with our data showing that LuxR interacts with

RNAP and has a binding site in the same location, indicates that this interaction and method of activation may be consistent in the small subset of TetR-type proteins that can act as activators. These similarities have led us to propose a mechanism for LuxR activation at $P_{luxCDABE}$ and other quorum sensing-regulated promoters that is similar to the mechanisms of CAP activation at class I and II promoters (Fig. 7): at class I promoters, CAP recruits RNAP, and at class II promoters, CAP both recruits and aids in open complex formation (Niu et al., 1996; Rhodius et al., 1997; Rhodius and Busby, 2000a; 2000b). Also of note, CAP has been shown to be able to interact with RNAP in the absence of promoter DNA with similar affinity as LuxR to RNAP (Heyduk et al., 1993). The ability of LuxR to bind RNAP in the absence of DNA, much like CAP (Fig. 1), indicates that LuxR likely has the ability to recruit RNAP to the promoter. Further, the positioning of LuxR binding site G as well as the LuxR-α NTD interaction indicates that LuxR may participate in open complex formation. Further investigation of the function of LuxR at both sites will serve to determine if our model is correct.

The $P_{luxCDABE}$ promoter is undoubtedly complex in regard to transcription regulation. Although LuxR binding sites A-G are all required for full activation at $P_{luxCDABE,}$ it is unclear what roles the majority of the binding sites are playing. We have shown that LuxR binding at site C drives an interaction with IHF and perhaps aids in IHF bending the DNA. LuxR binding to site E appears to block activation from the LCD transcription start site at high LuxR concentrations (Swartzman and Meighen, 1993; Chaparian et al., 2016). In addition to the seven LuxR binding sites, CAP was found to bind at $P_{luxCDABE}$. In strains deleted for cap, bioluminescence expression decreased 1000-fold (Chatterjee et al., 2002). This is especially interesting because CAP was another protein pulled down by LuxR in the FLAG-LuxR IP (Fig. 1A, Table S6), indicating it may also interact with LuxR. However, the exact role of CAP in the activation of $P_{luxCDABE}$ remains to be investigated.

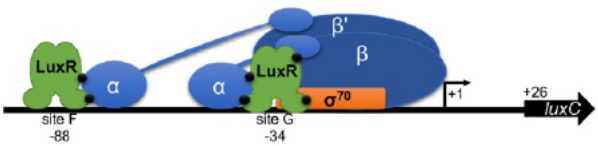

Fig. 7. Model of LuxR interaction with RNAP holoenzyme at the luxCDABE promoter in V. harveyi. LuxR binds to sites F and G in the luxCDABE promoter, which are centered at –88 and –34 relative to the primary transcription start site (small black arrow) respectively. LuxR binding facilitates recruitment of RNAP via interactions with the α subunit, both at the C-terminal domain (sites F and G) and N-terminal domain (site G). Putative sites of interaction between LuxR and RNAP are indicated by black circles. LuxR binding site G is positioned on top of the –35 site for σ^{70}, which may result in an interaction between LuxR and σ at this site. [Colour figure can be viewed at wileyonlinelibrary.com]

Further, the order of LuxR binding to each of the binding sites is unknown, as this may be driven by factors in addition to LuxR binding affinity for the site. There is no evidence of oligomerization of LuxR at any promoter, thus it appears that each binding site is independently bound by LuxR. At HCD, there are approximately 6500 dimers of LuxR in the cell, a sufficient amount to bind all 1165 LuxR binding sites identified in V. harveyi (van Kessel et al., 2013b). During the transition from LCD to HCD when the concentration of LuxR in the cell is increasing (~10-fold), the concentration of LuxR required to interact with proteins such as RNAP and IHF is not known. The delay of, or inability to, reach WT levels of bioluminescence expression by many of the luxR mutants in this study indicates that the LuxR interaction with RNAP is critical at this promoter. Our results show that these specific mutants do not have DNA-binding defects at sites F and G (Fig. 2C,D). Thus, collectively our data support the conclusion that LuxR interacts with RNAP via binding to sites F and G, placing LuxR in close proximity to RNAP.

Our data have also shown that RNAP interacts with multiple surface exposed α-helices of LuxR, and mutating the amino acids within these α-helices affects the ability of RNAP to bind to LuxR. Most mutations that we introduced in the LuxR interaction interface either had no effect or decreased LuxR's ability to activate at some promoters. The mutations that caused decreased LuxR activation suggest that these regions of LuxR are important for the function of LuxR in transcription activation. In particular, LuxR N142D and S76A were shown to decrease the ability of LuxR to activate at $P_{luxCDABE}$ and other quorum sensing-regulated genes, as well as have a decreased ability to bind α in vitro (Fig. 4F, Fig. 5B,D–F, Table 1), indicating that the decrease in LuxR activation is likely caused by an interruption of the LuxR-α interaction. Thus, we propose that the major interaction region of LuxR-RNAP is on LuxR α-helix 7 (L139 and N142), with another contributing region on α-helix 4 (S76) (Fig. 5A, Fig. 7). We also note that numerous mutations in the LuxR N-terminal loops and in α-helix 1 near the DNA-binding domains yielded activation defects. Although the effects of these mutations on RNAP interactions are difficult to tease apart from possible interruptions of DNA binding, some of these mutations (e.g. I4A) show wild-type levels of repression in vivo, suggesting that they are not affecting DNA binding at all sites. We propose that the LuxR-RNAP interaction interface also includes this N-terminal region and that this may play a role in interaction with the α CTD (Fig. 5A, Fig. 7).

The key residues 139 and 142 in the major LuxR-RNAP interaction region are conserved in vibrios (Fig. 6A) and are surface-exposed in the crystal structures of both HapR and SmcR (De Silva et al., 2007; Kim et al., 2010). Notably, none of these residues are involved in coordinating the ligand-binding pockets (Kim et al., 2018).

LuxR P8A, Q141A and N142I all displayed an increase in $P_{luxCDABE}$ activation, with LuxR Q141A and N142I displaying a moderate increase. The result from this experiment is intriguing because LuxR N142D displays a completely abrogated activation phenotype, indicating that the positively charge asparagine may be important at this interaction site, yet LuxR N142I lost this positive charge and displays an increased activation phenotype. In LuxR Q141A, the polar and hydrophobic amino acid, glutamine, is replaced with the nonpolar and hydrophilic amino acid, alanine. When considering both these variants, if an amino acid in this area plays either no role or an opposing role in this interaction is changed to an amino acid that instead contributes to the interaction, or is simply more hydrophobic, the mutant LuxR protein could interact more strongly with RNAP. Regarding the LuxR P8A mutation, it displayed an increased ability to activate at $P_{luxCDABE}$ compared to wild-type LuxR in the beginning stages of LuxR expression. As LuxR P8A induction progresses, the relative expression of bioluminescence decreases compared to wild-type LuxR and remains lower than wild-type levels at the end of the curve (Fig 5B). It is possible that the amino acid structural change in LuxR P8A is advantageous for binding to a more 'naked' promoter early in the transition from LCD to HCD but eventually becomes a hindrance to activation.

Notably, our data show that the LuxR-RNAP interaction is conserved across vibrios. When the analogous LuxR S76A and N142D mutations were made in the V. cholerae LuxR homolog, HapR, an activation-deficient phenotype was observed not only at $P_{luxCDABE}$ but also on the V. cholerae quorum sensing-regulated gene hapA. This indicates that the LuxR/HapR-RNAP interaction is necessary for quorum sensing gene expression in not only V. harveyi but also in V. cholerae and likely across the Vibrio genus.

It is important to note that the activation-defective phenotypes of the LuxR mutant proteins could be caused by something in addition to an alteration in their ability to interact with RNAP. For example, it has been shown that LuxR and IHF synergistically bind to the $P_{luxCDABE}$ promoter, IHF is required for full activation of $P_{luxCDABE}$, and LuxR interacts with IHF in vitro (Chaparian et al., 2016). Our LuxR IP also identified an interaction between LuxR and IHF in vivo. Thus, it is possible that a LuxR activation-deficient mutant could retain a wild-type level of interaction with RNAP and instead be altered in its ability to interact with other proteins such as IHF (e.g. LuxR I4A and L139R which were not significantly altered in interaction with α in BLI experiments).

Our current model for LuxR-RNAP interaction-mediated activation at the $P_{luxCDABE}$ promoter is presented in Fig. 7. We propose that LuxR interacts with the α-CTD at promoters in which there are LuxR binding sites >60 but <100 bp upstream of the transcription start site. We also propose that LuxR interacts with the α-CTD, α-NTD, and possibly σ^{70} at promoters in which there are LuxR binding sites that overlap with the –35 element. While this fits the biochemical and genetic data for the $P_{luxCDABE}$ promoter, not all LuxR-activated promoters fit these promoter architecture descriptions, indicating there is likely a RNAP interaction-independent mode of LuxR activation. The mechanism for how LuxR activates at promoters where its binding sites are not within range of interaction with the α-subunit of RNAP remains to be investigated.

Surprisingly, despite stringent washes and conditions, our in vivo FLAG-LuxR IP indicated that LuxR interacts with hundreds of other proteins (Fig. 1A, Tables S4–S6). This high volume of potential LuxR interacting proteins may be due to that 'sticky' area on LuxR alpha helix 4 discovered in the control peptide array (Fig. 4D). Even so, many of the identified proteins seem like legitimate LuxR interaction partners. As we have shown, LuxR interacts with RNAP and in this experiment every subunit of RNAP was pulled down, including many sigma factors that may interact with LuxR or simply have been pulled down via their interaction with the core enzyme. Many of the proteins pulled down in association with LuxR are transcription factors, and direct interactions between transcription factors that aid in activation or repression is not uncommon. Several of the proteins pulled down were nucleoid-associated proteins including IHF, which has been validated as an interaction partner with LuxR (Chaparian et al., 2016). Whether or not many of these proteins are bona fide LuxR interaction partners and their possible role in transcription regulation remains to be determined.

Experimental procedures

Bacterial strains and media

The E. coli strains S17-1λpir and DH10B were used for cloning purposes, and the E. coli BL21 (DE3) strain was used for protein expression. E. coli strains were grown at 30°C or 37°C shaking at 275 RPM in Lysogeny Broth (LB) medium supplemented with 40 μg ml^{-1} kanamycin 100 μg ml^{-1} ampicillin, and 10 μg ml^{-1} chloramphenicol as required. The strain of V. harveyi is BB120 (BAA-1116), which was recently reclassified as Vibrio campbellii BAA-1116 (Lin et al., 2010). For consistency with the plethora of literature with BB120, we have referred to this strain as V. harveyi throughout the manuscript. BB120 and derivatives were grown at 30°C in Luria Marine (LM) medium supplemented with 250 μg ml^{-1} kanamycin and either 5 μg ml^{-1} or 10 μg ml^{-1} chloramphenicol as required. Plasmids were transferred from E. coli to V. harveyi strains by conjugation on LB plates, and exconjugants were selected on LM plates with polymyxin B at 50 U ml^{-1} and the appropriate selective antibiotic. V. cholerae strain AC53 and derivatives were grown at 30°C in LB

medium supplemented 40 μg ml^{-1} kanamycin and 5 μg ml^{-1} or 10 μg ml^{-1} tetracyclin (liquid and agar medium respectively) as required. The SAD793 strain containing the mutation in hapR was constructed as previously described using natural transformation of splicing-by-overlap extension PCR products by natural transformation (Dalia et al., 2013). All strains were verified by PCR and sequencing.

Molecular methods and statistical analyses

PCR was performed using Phusion HF polymerase (New England Biolabs). Restriction enzymes and enzymes for isothermal DNA assembly (Gibson et al., 2009) (T5 exo, Q5 polymerase, Taq ligase) were purchased from New England Biolabs. Phusion HF polymerase was used for site-directed mutagenesis PCR following the QuikChange mutagenesis (Stratagene) protocol. All oligonucleotides were ordered from Integrated DNA Technologies. Sequencing of plasmids/PCR products was conducted at ACGT or Eurofins Scientific. Plasmid cloning procedures and PCR primer sequences are available upon request. DNA samples were resolved on 1% agarose gels, and protein samples were resolved on 12%, 15% or 4–20% gradient SDS-PAGE gels. RNA extraction and qRT-PCR experiments were performed as described with cells collected at OD_{600} = 1.0 (Chaparian et al., 2016). The $\Delta\Delta C_T$ method was used to analyze data normalized to hfq as the internal standard gene for V. harveyi or rpoB for V. cholerae.

Unless otherwise noted, data are plotted for triplicate independent experiments. Symbols on graphs represent the mean values, and error bars are standard deviations. Statistical analyses were performed with GraphPad Prism version 7.0c. Additional information about statistical analyses is included in the figure legends.

Fluorescence and bioluminescence assays

Bioluminescence and fluorescence assays were performed in strains containing plasmids with luxR expressed under control of the IPTG-inducible P_{tac} promoter and lacIq system. For bioluminescence assays, overnight cultures of V. harveyi or V. cholerae were diluted to OD_{600} = 0.05 in fresh LM media or LB media, respectively, containing selective antibiotic and 10 μM IPTG (V. harveyi) or 1 μM IPTG (V. cholerae) in 200 μl in 96-well plates. The plate was incubated shaking at 30°C for 24 h in a BioTek Synergy H1 plate reader with bioluminescence and OD_{600} readings taken every 30 min. For fluorescence assays to measure GFP and mCherry expression, E. coli cultures containing LuxR expression plasmids were grown shaking at 30°C for 16 h, and 200 μl of the cultures was measured in 96-well plates for GFP, mCherry and OD_{600} in a BioTek Synergy H1 plate reader.

Immunoprecipitation assays

LuxR immunoprecipitation (IP) assays were performed with a ΔluxR V. harveyi strain (KM669) containing plasmids expressing either FLAG-LuxR (pAP116) from the native luxR promoter, FLAG-LuxR R17C (pST012) from the native luxR promoter or empty vector (pSLS3). The strain was inoculated in 25 ml LM at a dilution of 1:25 and grown shaking at 30°C for 16 h overnight. To prepare lysates, 50 OD_{600} units of cells were pelleted, 1 ml lysis buffer (1 ml BugBuster® (Millipore Sigma), 1× protease inhibitors (Sigma-Aldrich), 0.15 mg ml^{-1} lysozyme, 0.01% Triton X-100, 1 mM PMSF, 100 mM NaCl, 50 mM HEPES–KOH pH 7.5, 10 mM $MgCl_2$, 0.08 mg ml^{-1} DNase) was added, and this mixture was incubated rotating at room temperature (RT) for 20 min. Lysates were clarified by centrifuging at 13000 × g for 10 min. ANTI-FLAG® M2 Affinity Gel (Sigma-Aldrich) was washed 3 times with IP buffer. At RT, 400 μl IP buffer (50 mM HEPES-KOH pH 7.5, 0.5 mM EDTA, 0.1% Triton X-100, 500 mM NaCl, 1 mM PMSF) and 10 μl ANTI-FLAG® M2 Affinity Gel were added to 100 μl of lysate and incubated 1 h rotating at RT. The affinity gel was washed with 500 μl IP buffer while rotating for 5 min 3 times. To elute proteins from the affinity gel, 25 μl of 6× Sample Buffer (0.5 M Tris–HCl pH 6.8, 6.4% SDS, 6% β-mercaptoethanol, 12% glycerol, 6 mg Bromophenol blue) was added to the beads and boiled at 95°C for 5 min. Proteins were resolved on a 15% SDS-PAGE gel, and select gel slices containing sample were analyzed by the Laboratory for Biological Mass Spectrometry at Indiana University. The control sample lane was sent in its entirety, whereas the FLAG-LuxR sample lane was cut into three segments for processing (top, middle, bottom; see Tables S4–S6).

Mass spectrometry

Gel bands were diced into 1 mm cubes and incubated for 45 min at 57°C with 2.1 mM dithiothreitol to reduce cysteine residue side chains. These side chains were then alkylated with 4.2 mM iodoacetamide for 1 h in the dark at 21°C. A solution containing 1 μg trypsin in 25 mM ammonium bicarbonate was added and the samples were digested for 12 h at 37°C. The resulting peptides were desalted using a ZipTip (Millipore, Billerica, MA). The samples were dried down and injected into an Eksigent HPLC coupled to a LTQ Velos mass spectrometer (Thermo Fisher Scientific, Waltham, MA) operating in 'top five' data-dependent MS/MS selection. The peptides were separated using a 75 micron, 15 cm column packed in-house with C18 resin (Michrom Bioresources, Auburn, CA) at a flow rate of 300 nl min^{-1}. A 1 h gradient was run from Buffer A (2% acetonitrile, 0.1% formic acid) to 60% Buffer B (100% acetonitrile, 0.1% formic acid).

Co-immunoprecipitation assays

FLAG-LuxR and His-RNAP were incubated in a 4:1 ratio at 7.2 μM:1.8 μM, respectively, with 333 nM RNAP binding DNA substrate (substrate generated by PCR with oligos AB052, AB053) in 30 μl reactions in co-IP buffer (50 mM HEPES pH 7.5, 200 mM NaCl, 0.1% Triton X-100). The reactions were incubated for 30 min at RT. Subsequently, 10 μl of ANTI-FLAG® M2 Affinity Gel (Sigma-Aldrich) (to immunoprecipitate FLAG-LuxR) or HIS-Select® Nickel Affinity Gel (Sigma) (to immunoprecipitate His-RNAP) were washed 3

times in co-IP buffer and then added to the reactions and incubated for 30 min at RT rotating. The reactions were washed 3 times in co-IP for 5 min rotating. To elute proteins from the gel, 20 µl of 2% SDS was added and boiled for 5 min at 95°C. Samples were analyzed on 12% SDS-PAGE gels. These gels were either stained with coomassie brilliant blue stain or further analyzed by western blot.

Western blots

Proteins from SDS-PAGE gels were transferred to a 0.45-µm nitrocellulose membrane by wet transfer in Transfer Buffer (48 mM Tris Base, 39 mM Glycine, 0.037% SDS, 20% methanol) for 60–70 min at 500 mA. Membranes were blocked overnight in a 5% milk/TBS-T solution (5 g nonfat dry milk per 100 ml buffer, 25 mM Tris-Cl pH 8.0, 125 mM NaCl 0.1% Tween 20). The membrane was washed 3 times with TBS-T rocking for 5 min and subsequently incubated with anti-FLAG-HRP primary antibody (Sigma, 1:5,000), anti-His-HRP primary antibody (Sigma, 1:3,000), primary antibodies against RNAP subunits (α1:10,000;β,β′, σ, 1:1,000; all from Neoclone) or primary antibodies against LuxR (1:3000) for 1 h at RT. All primary incubations were performed in TBS-T except incubations with anti-LuxR antibodies, which were incubated with 5% milk in TBS-T. Membranes were washed 3 times with TBS-T rocking for 5 min and, when necessary, incubated with anti-mouse or anti-rabbit HRP-conjugated secondary antibody (1:10,000, Promega) for 30 min at RT. Membranes were washed 3 times with TBS-T rocking for 5 min, treated with Pierce® ECL Western Blotting Substrate (Thermo Scientific) for 5 min and exposed to film.

Protein purification

The His-RNAP core enzyme purification plasmid pAI900 was a generous gift from the Richard Gourse lab. It expresses α, β, β′ and ω subunits with a C-terminal H10x His-tag on β′. An overnight culture of BL21(DE3) cells containing pAI900 was diluted 1:100 into 1 L fresh LB with 100 µg ml^{-1} ampicillin medium and grown at 30°C until OD_{600} reached 0.5–0.6. Expression of His-RNAP was induced with 1 mM IPTG, followed by growth for 3 h at 30°C. Cells were pelleted at 4,000 × g for 10 min at 4°C, and the pellet was resuspended in 2 ml lysis buffer per gram of pellet (1 ml BugBuster® (Millipore Sigma), 1× protease inhibitors, 0.15 mg ml^{-1} lysozyme, 0.01% Triton X-100, 1 mM PMSF, 100 mM NaCl, 50 mM HEPES-KOH pH 7.5, 10 mM $MgCl_2$, 0.08 mg ml^{-1} DNase) and incubated at 4°C rocking for 30 min. The lysate was clarified at 14,000 × g for 20 min at 4°C. The lysate was applied to a HisTrap™ column (GE Healthcare) on an Akta Pure L, washed with 20 column volumes of HisTrap RNAP Buffer A (50 mM Na_2HPO_4, 0.3 M NaCl, 30 mM imidazole, 0.1% Tween 20, 5% ethanol, 5 mM β-mercaptoethanol) and eluted with HisTrap RNAP Buffer B (50 mM Na_2HPO_4, 0.3 M NaCl, 300 mM Imidazole, 0.1% Tween 20, 5% Ethanol, 5 mM β-mercaptoethanol). The eluted fractions were pooled and applied to a HiTrap™ Heparin HP column (GE Healthcare), washed with 20 column volumes of RNAP Heparin Buffer A (10 mM Tris–HCl pH 8, 0.1 mM EDTA, 5% glycerol, 0.2 M NaCl), and eluted with RNAP Heparin Buffer B (10 mM Tris–HCl pH 8, 0.1 mM EDTA, 5% glycerol, 0.6 M NaCl). The fractions were pooled and dialyzed overnight at 4°C in RNAP Storage Buffer (10 mM Tris–HCl pH 8.0, 100 mM KCl, 10 mM $MgCl_2$, 0.1 mM EDTA, 50% Glycerol, 0.5 mM DTT). Purified RNAP was flash frozen on liquid N_2 and stored at –80°C.

The His-α purification plasmid pRLG3538 (N-terminal 6× His-tagged WT α subunit) and pRLG3657 His-α Δ235 (N-terminal 6xHis-tagged with a C-terminal truncation, expressing α 1-234) were also generous gifts from the Gourse lab. An overnight culture of BL21(DE3) cells containing pRLG3538 or pRLG3657 were diluted 1:100 into 1 L fresh LB medium with 100 µg ml^{-1} ampicillin and grown at 37°C until OD_{600} reached 0.5–0.6. Expression of His-α or His-α Δ235 was induced with 1 mM IPTG and incubated shaking 3 h at 37°C. The cells were pelleted at 4,000×g for 10 min at 4°C. The pellet was resuspended in 2 ml lysis buffer per gram of pellet or lysed using an Avestin EmulsiFlex-C3 and incubated at 4°C rocking for 30 min. The lysate was clarified by centrifuging at 14,000 × g for 20 min at 4°C. The lysate was applied to a HisTrap™ column (GE Healthcare), washed with 20 column volumes of Alpha Buffer A (20mM Tris pH 8.0, 500mM NaCl 5mM imidazole) and eluted with Alpha Buffer B (20mM Tris pH 8.0, 500mM NaCl 500mM imidazole). The eluted fractions were pooled and applied to a HiPrep™ Sephacryl S200 (16/60) column (GE Healthcare) using gel filtration buffer (10 mM Tris–HCl pH 8.0, 100 mM KCl, 10 mM $MgCl_2$, 0.1 mM EDTA). The fractions were pooled and dialyzed overnight at 4°C in RNAP storage buffer. Aliquots of purified His-α and His-α Δ235 were flash frozen on liquid N_2 and stored at –80°C.

LuxR, His-LuxR and FLAG-LuxR were purified as previously described (Chaparian et al., 2016) from BL21(DE3) cells containing either pJV079 (wild-type LuxR), pJV080 (His-LuxR), or pJV143 (FLAG-LuxR).

Purification of His-TEV protease was performed using plasmid pMHT238Δ (Blommel and Fox, 2007), which is an engineered TEV protease lacking C-terminal residues 238-242. Plasmid pMHT238Δ was transformed into B834(DE3)::pRIL cells, and colonies were inoculated into 1 ml LB media with kanamycin and chloramphenicol grown shaking at 37°C for 3 h. These cultures were added to 25 ml of fresh selective medium and grown shaking at 37°C for 2 h. Finally, the two 25 ml cultures were used to inoculate two 1 L cultures of fresh selective medium and grown shaking at 37°C for 3 h. The culture was moved to 18°C shaking for 30 min, 0.5 mM IPTG added and incubated shaking at 18°C for 15.5 h. The cells were pelleted and resuspended in lysis buffer (25 mM Na_2HPO_4, 25 mM NaH_2PO_4, pH 7.8, 1 M NaCl, 30 mM imidazole, 20 µg ml^{-1} DNaseI and 1X protease inhibitors (Sigma)). Fastbreak (Promega) was added at 1X concentration for 15 min stirring at room temperature. Insoluble material was pelleted at 15,000 RPM for 30 min at 4°C. The lysate was applied to a HisTrap™ FF column (GE Healthcare) equilibrated with column buffer (25 mM Na_2HPO_4, 25 mM NaH_2PO_4, pH 7.8, 1 M NaCl, 30 mM imidazole), washed with 20 column volumes of column buffer and eluted with 5 column volumes of elution buffer (25 mM Na_2HPO_4, 25 mM NaH_2PO_4, pH 7.8, 1 M NaCl, 0.5 M imidazole). Fractions containing His-TEV protease were collected, dialyzed into

final buffer (25 mM Na_2HPO_4, 25 mM NaH_2PO_4, pH 7.8, 1 M NaCl, 2 mM DTT, 20% glycerol), flash frozen on liquid N_2 and stored at –80°C.

Electrophoretic mobility shift assays

EMSAs were performed as described (van Kessel et al., 2013b). For analyses of LuxR protein binding affinities, the amount of probe shifted was quantified compared to unbound probe using ImageJ software. Background density (determined by reactions lacking LuxR protein) was subtracted from the densities of shifted probe bands. Percent DNA bound was calculated as the fraction of shifted probe divided by the total density from shifted and unshifted probe. Binding affinities and statistical analyses were performed on GraphPad Prism version 7.0c.

Bio-layer interferometry

Bio-layer interferometry was performed on an Octet® K2 System using Dip and Read™ Ni-NTA (NTA) Biosensors (FortéBio®). In a 96-well plate, the following reactions were prepared: (i) a reference well containing BLI Buffer (1× Kinetics Buffer™ (FortéBio®) diluted in PBS (Sigma)), 200 mM NaCl, 0.05% Tween 20), (ii) a ligand-loading well containing 200 nM E. coliα, E. coli ΔCTDα,V. harveyiα or tobacco etch virus TEV protease (i.e. the ligand) in BLI buffer and (iii) an association well containing the V. harveyi LuxR or various LuxR mutant proteins (i.e. the analyte) at various concentrations (1000, 850, 700, 550, 400, 250 and 0 nM). The method on the Octet® K2 System data acquisition software was set to perform a 30 s sensor check in the reference well, 600 s ligand-loading step in the ligand-loading well, 60 s baseline step in the reference well, 700 s association step in the association well, and 700 s dissociation step in the reference well. All steps were performed shaking at RT for each concentration of analyte. The data were analyzed using Octet® K2 System data analysis software.

LuxR peptide array

A LuxR peptide array was designed and produced by Kinexus Bioinformatics Corp. The array consisted of the entire primary amino acid sequence of LuxR synthesized in 10 amino acid segments each shifted by 3 amino acids with 7 amino acids of overlap between segments. The peptide array membrane was hydrated with 100% methanol for 10 min, washed in TBS for 5 min 3 times and blocked in 5% milk/TBS-T rocking overnight at 4°C. The membrane was washed once in TBS-T for 5 min rocking at RT. The membrane was incubated with 5 μg ml^{-1} E. coli His-RNAP, 0.8 μg ml^{-1} V. harveyi α subunit or 0.8 μg ml^{-1} tobacco etch virus TEV protease in TBS-T for 3 h. The membrane was washed 3 times in TBS-T for 5 min with rocking. The membrane was incubated with 5 ml TBS-T/anti-β′ antibody (1:1,000) or 10 ml TBS-T/anti-α antibody (1:10,000) for 1.5 h or 15 ml TBS-T/anti-His antibody for 2 h, washed 3 times in TBS-T for 5 min, incubated with the anti-mouse secondary (1:1,000) for 1 h when applicable, and washed 3 times in TBS-T for 5 min. The membrane was incubated with Pierce® ECL Western Blotting Substrate (Thermo Scientific) for 2 min and then exposed to film.

Acknowledgements

The authors wish to acknowledge Trevor Douglas for allowing us to use the Octet system and Sundhar Subramanian for assistance with BLI experiments and data analysis. We also thank Jonathan Trinidad and the Indiana University Laboratory for Biological Mass Spectrometry for analysis of protein samples. We gratefully thank Richard Gourse and Wilma Ross for generously providing RNA polymerase expression plasmids, strains and guidance on experiments. We thank Jared Cochran for sharing the His-TEV protease plasmid-containing E. coli strain and Susanne Ressl and Jane Newman for assistance with PyMol image generation. The V. cholerae strains and rpoB primers were generously provided by Ankur Dalia. We thank Chelsea Simpson for excellent technical assistance and Clay Fuqua and Matt Bochman for comments on the manuscript. This work was supported by National Institutes of Health (NIH) grant 1R35GM124698-01 to JVK.

Conflict of interest

The authors declare that that they have no conflicts of interest to declare.

Author contributions

AB and JVK designed and carried out experiments, analyzed and interpreted data, and wrote this manuscript.

References

Ball, A.S., Chaparian, R.R. and van Kessel, J.C. (2017) Quorum sensing gene regulation by LuxR/HapR master regulators in Vibrios. Journal of Bacteriology, **199**, e00105-17.

Bell, A., Gaston, K., Williams, R., Chapman, K., Kolb, A., Buc, H. et al. (1990) Mutations that alter the ability of the Escherichia coli cyclic AMP receptor protein to activate transcription. Nucleic Acids Research, **18**, 7243–7250.

Blommel, P.G. and Fox, B.G. (2007) A combined approach to improving large-scale production of tobacco etch virus protease. Protein Expression and Purification, **55**, 53–68.

Bokal, A.J., Ross, W. and Gourse, R.L. (1995) The transcriptional activator protein FIS: DNA interactions and cooperative interactions with RNA polymerase at the Escherichia coli rrnB P1 promoter. Journal of Molecular Biology, **245**, 197–207.

Chaparian, R.R., Olney, S.G., Hustmyer, C.M., Rowe-Magnus, D.A. and van Kessel, J.C. (2016) Integration host factor and LuxR synergistically bind DNA to coactivate quorum-sensing genes in Vibrio harveyi. Molecular Microbiology, **101**, 823–840.

Chatterjee, J., Miyamoto, C.M. and Meighen, E.A. (1996) Autoregulation of luxR: the Vibrio harveyi lux-operon activator functions as a repressor. Molecular Microbiology, **20**, 415–425.
Chatterjee, J., Miyamoto, C.M., Zouzoulas, A., Lang, B.F., Skouris, N. and Meighen, E.A. (2002) MetR and CRP bind to the Vibrio harveyi lux promoters and regulate luminescence. Molecular Microbiology, **46**, 101–111.
Christen, S., Srinivas, A., Bahler, P., Zeller, A., Pridmore, D., Bieniossek, C. et al. (2006) Regulation of the Dha operon of Lactococcus lactis: a deviation from the rule followed by the Tetr family of transcription regulators. Journal of Biological Chemistry, **281**, 23129–23137.
Dalia, A.B., Lazinski, D.W. and Camilli, A. (2013) Characterization of undermethylated sites in Vibrio cholerae. Journal of Bacteriology, **195**, 2389–2399.
De Silva, R.S., Kovacikova, G., Lin, W., Taylor, R.K., Skorupski, K. and Kull, F.J. (2007) Crystal structure of the Vibrio cholerae quorum-sensing regulatory protein HapR. Journal of Bacteriology, **189**, 5683–5691.
Fidopiastis, P.M., Miyamoto, C.M., Jobling, M.G., Meighen, E.A. and Ruby, E.G. (2002) LitR, a new transcriptional activator in Vibrio fischeri, regulates luminescence and symbiotic light organ colonization. Molecular Microbiology, **45**, 131–143.
Gaston, K., Bell, A., Kolb, A., Buc, H. and Busby, S. (1990) Stringent spacing requirements for transcription activation by CRP. Cell, **62**, 733–743.
Gibson, D.G., Young, L., Chuang, R.Y., Venter, J.C., Hutchison, C.A. 3rd and Smith, H.O. (2009) Enzymatic assembly of DNA molecules up to several hundred kilobases. Nature Methods, **6**, 343–345.
Hawver, L.A., Jung, S.A. and Ng, W.L. (2016) Specificity and complexity in bacterial quorum-sensing systems. FEMS Microbiology Reviews, **40**, 738–752.
Heyduk, E. and Heyduk, T. (1993) Physical studies on interaction of transcription activator and RNA-polymerase: fluorescent derivatives of CRP and RNA polymerase. Cellular and Molecular Biology Research, **39**, 401–407.
Heyduk, T., Lee, J.C., Ebright, Y.W., Blatter, E.E., Zhou, Y. and Ebright, R.H. (1993) CAP interacts with RNA polymerase in solution in the absence of promoter DNA. Nature, **364**, 548–549.
Igarashi, K., Hanamura, A., Makino, K., Aiba, H., Aiba, H., Mizuno, T. et al. (1991) Functional map of the alpha subunit of Escherichia coli RNA polymerase: two modes of transcription activation by positive factors. Proceedings of the National Academy of Sciences of the United States of America, **88**, 8958–8962.
Ishihama, A. (1992) Role of the RNA polymerase alpha subunit in transcription activation. Molecular Microbiology, **6**, 3283–3288.
Jeong, H.S., Kim, S.M., Lim, M.S., Kim, K.S. and Choi, S.H. (2010) Direct interaction between quorum-sensing regulator SmcR and RNA polymerase is mediated by integration host factor to activate vvpE encoding elastase in Vibrio vulnificus. Journal of Biological Chemistry, **285**, 9357–9366.
Jobling, M.G. and Holmes, R.K. (1997) Characterization of hapR, a positive regulator of the Vibrio cholerae HA/protease gene hap, and its identification as a functional homologue of the Vibrio harveyi luxR gene. Molecular Microbiology, **26**, 1023–1034.
van Kessel, J.C., Rutherford, S.T., Shao, Y., Utria, A.F. and Bassler, B.L. (2013a) Individual and combined roles of the master regulators AphA and LuxR in control of the Vibrio harveyi quorum-sensing regulon. Journal of Bacteriology, **195**, 436–443.
van Kessel, J.C., Ulrich, L.E., Zhulin, I.B. and Bassler, B.L. (2013b) Analysis of activator and repressor functions reveals the requirements for transcriptional control by LuxR, the master regulator of quorum sensing in Vibrio harveyi. mBio, **4**, e00378-13.
van Kessel, J.C., Rutherford, S.T., Cong, J.P., Quinodoz, S., Healy, J. and Bassler, B.L. (2015) Quorum sensing regulates the osmotic stress response in Vibrio harveyi. Journal of Bacteriology, **197**, 73–80.
Kim, Y., Kim, B.S., Park, Y.J., Choi, W.C., Hwang, J., Kang, B.S. et al. (2010) Crystal structure of SmcR, a quorum-sensing master regulator of Vibrio vulnificus, provides insight into its regulation of transcription. Journal of Biological Chemistry, **285**, 14020–14030.
Kim, B.S., Jang, S.Y., Bang, Y.J., Hwang, J., Koo, Y., Jang, K.K. et al. (2018) QStatin, a selective inhibitor of quorum sensing in Vibrio species, mBio, **9**, e02262-17.
Lee, D.J., Minchin, S.D. and Busby, S.J. (2012) Activating transcription in bacteria. Annual Review of Microbiology, **66**, 125–152.
Lin, B., Wang, Z., Malanoski, A.P., O'Grady, E.A., Wimpee, C.F., Vuddhakul, V. et al. (2010) Comparative genomic analyses identify the Vibrio harveyi genome sequenced strains BAA-1116 and HY01 as Vibrio campbellii. Environmental Microbiology Reports, **2**, 81–89.
Lo Scrudato, M. and Blokesch, M. (2013) A transcriptional regulator linking quorum sensing and chitin induction to render Vibrio cholerae naturally transformable. Nucleic Acids Research, **41**, 3644–3658.
Metzger, L.C., Stutzmann, S., Scrignari, T., Van der Henst, C., Matthey, N. and Blokesch, M. (2016) Independent regulation of type VI secretion in Vibrio cholerae by TfoX and TfoY. Cell Reports, **15**, 951–958.
Ng, W.L. and Bassler, B.L. (2009) Bacterial quorum-sensing network architectures. Annual Review of Genetics, **43**, 197–222.
Niu, W., Zhou, Y., Dong, Q., Ebright, Y.W. and Ebright, R.H. (1994) Characterization of the activating region of Escherichia coli catabolite gene activator protein (CAP). I. Saturation and alanine-scanning mutagenesis. Journal of Molecular Biology, **243**, 595–602.
Niu, W., Kim, Y., Tau, G., Heyduk, T. and Ebright, R.H. (1996) Transcription activation at class II CAP-dependent promoters: two interactions between CAP and RNA polymerase. Cell, **87**, 1123–1134.
Pompeani, A.J., Irgon, J.J., Berger, M.F., Bulyk, M.L., Wingreen, N.S. and Bassler, B.L. (2008) The Vibrio harveyi master quorum-sensing regulator, LuxR, a TetR-type protein is both an activator and a repressor: DNA recognition and binding specificity at target promoters. Molecular Microbiology, **70**, 76–88.
Pribnow, D. (1975) Nucleotide sequence of an RNA polymerase binding site at an early T7 promoter. Proceedings

of the National Academy of Sciences of the United States of America, **72**, 784–788.
Ramos, J.L., Martinez-Bueno, M., Molina-Henares, A.J., Teran, W., Watanabe, K., Zhang, X. et al. (2005) The TetR family of transcriptional repressors. Microbiology and Molecular Biology Reviews, **69**, 326–356.
Rhodius, V.A. and Busby, S.J. (2000a) Interactions between activating region 3 of the Escherichia coli cyclic AMP receptor protein and region 4 of the RNA polymerase sigma(70) subunit: application of suppression genetics. Journal of Molecular Biology, **299**, 311–324.
Rhodius, V.A. and Busby, S.J. (2000b) Transcription activation by the Escherichia coli cyclic AMP receptor protein: determinants within activating region 3. Journal of Molecular Biology, **299**, 295–310.
Rhodius, V.A., West, D.M., Webster, C.L., Busby, S.J. and Savery, N.J. (1997) Transcription activation at class II CRP-dependent promoters: the role of different activating regions. Nucleic Acids Research, **25**, 326–332.
Robert, X. and Gouet, P. (2014) Deciphering key features in protein structures with the new ENDscript server. Nucleic Acids Research, **42**, W320–W324.
Rutherford, S.T. and Bassler, B.L. (2012) Bacterial quorum sensing: its role in virulence and possibilities for its control. Cold Spring Harbor Perspectives in Medicine, **2**, a012427.
Savery, N.J., Lloyd, G.S., Kainz, M., Gaal, T., Ross, W., Ebright, R.H. et al. (1998) Transcription activation at class II CRP-dependent promoters: identification of determinants in the C-terminal domain of the RNA polymerase alpha subunit. EMBO Journal, **17**, 3439–3447.
Savery, N.J., Lloyd, G.S., Busby, S.J., Thomas, M.S., Ebright, R.H. and Gourse, R.L. (2002) Determinants of the C-terminal domain of the Escherichia coli RNA polymerase alpha subunit important for transcription at class I cyclic AMP receptor protein-dependent promoters. Journal of Bacteriology, **184**, 2273–2280.
Sievers, F., Wilm, A., Dineen, D., Gibson, T.J., Karplus, K., Li, W. et al. (2011) Fast, scalable generation of high-quality protein multiple sequence alignments using Clustal Omega. Molecular Systems Biology, **7**, 539.
Studer, S.V., Mandel, M.J. and Ruby, E.G. (2008) AinS quorum sensing regulates the Vibrio fischeri acetate switch. Journal of Bacteriology, **190**, 5915–5923.
Svenningsen, S.L., Waters, C.M. and Bassler, B.L. (2008) A negative feedback loop involving small RNAs accelerates Vibrio cholerae's transition out of quorum-sensing mode. Genes & Development, **22**, 226–238.
Swartzman, E. and Meighen, E.A. (1993) Purification and characterization of a poly(dA-dT) lux-specific DNA-binding protein from Vibrio harveyi and identification as LuxR. Journal of Biological Chemistry, **268**, 16706–16716.
Swartzman, E., Silverman, M. and Meighen, E.A. (1992) The luxR gene product of Vibrio harveyi is a transcriptional activator of the lux promoter. Journal of Bacteriology, **174**, 7490–7493.
Tang, H., Severinov, K., Goldfarb, A. and Ebright, R.H. (1995) Rapid RNA polymerase genetics: one-day, no-column preparation of reconstituted recombinant Escherichia coli RNA polymerase. Proceedings of the National Academy of Sciences of the United States of America, **92**, 4902–4906.
Tsou, A.M., Cai, T., Liu, Z., Zhu, J. and Kulkarni, R.V. (2009) Regulatory targets of quorum sensing in Vibrio cholerae: evidence for two distinct HapR-binding motifs. Nucleic Acids Research, **37**, 2747–2756.
Waters, C.M. and Bassler, B.L. (2006) The Vibrio harveyi quorum-sensing system uses shared regulatory components to discriminate between multiple autoinducers. Genes & Development, **20**, 2754–2767.
Zheng, J., Ho, B. and Mekalanos, J.J. (2011) Genetic analysis of anti-amoebae and anti-bacterial activities of the type VI secretion system in Vibrio cholerae. PLoS One, **6**, e23876.
Zhou, Y., Merkel, T.J. and Ebright, R.H. (1994a) Characterization of the activating region of Escherichia coli catabolite gene activator protein (CAP). II. Role at class I and class II CAP-dependent promoters. Journal of Molecular Biology, **243**, 603–610.
Zhou, Y., Pendergrast, P.S., Bell, A., Williams, R., Busby, S. and Ebright, R.H. (1994b) The functional subunit of a dimeric transcription activator protein depends on promoter architecture. EMBO Journal, **13**, 4549–4557.

Supporting Information

Additional supporting information may be found online in the Supporting Information section at the end of the article.